

Supplemental material

Late spring bloom development of pelagic diatoms in Baffin Bay

Augustin Lafond¹, Karine Leblanc¹, Bernard Quéguiner¹, Brivaela Moriceau², Aude Leynaert²,
Véronique Cornet¹, Justine Legras¹, Joséphine Ras⁴, Marie Parenteau³, Nicole Garcia¹, Marcel Babin³,
Jean-Éric Tremblay³.

¹ Aix-Marseille Univ., Université de Toulon, CNRS, IRD, MIO, UM110, Marseille, 13288, France

² Laboratoire des Sciences de l'Environnement Marin, UMR CNRS 6539, Institut Universitaire
Européen de la Mer, Technopole Brest-Iroise, Plouzané, France

³ Takuvik Joint International Laboratory, Laval University (Canada), CNRS, FR; Département de
biologie et Québec-Océan, Université Laval, Québec, CA

⁴ Sorbonne Universités, UPMC Univ Paris 06, CNRS, IMEV, Laboratoire d'Océanographie de
Villefranche UMR7093, 06230, Villefranche-sur-mer, France

Correspondance : Augustin Lafond (augustin.lafond@gmail.com)

List of Tables and Figures

Table S1: Linear measurements, biovolume, and carbon biomass of the taxa observed in Baffin Bay.....	3
Table S2: Functional trait data for the taxa observed in Baffin Bay	3
Table S3: Summary of the environmental and biological data at the 29 stations.....	5
Table S4: Diatoms observed in Baffin Bay during the Green Edge expedition	6
Figure S1: Selection of diatom species observed by scanning electron microscopy (SEM).....	7
Figure S2: T-S diagram for all of the stations	8
Figure S3: Vertical distribution of concentrations of chlorophyll <i>a</i> and nutrients (nitrate, orthosilicic acid, and phosphate) for transect T3	9
Figure S4: Integrated nutrient concentrations over the depth of the equivalent mixed layer (hBD).....	10
Figure S5: Potential limiting nutrients in rank order (most limiting first) based on nutrient ratios.....	11
Figure S6: Abundance of <i>Phaeocystis</i> spp. in surface waters and at the subsurface chlorophyll <i>a</i> maximum .	12
Figure S7: Examples of actively silicifying diatoms labelled with the fluorescent dye PDMPO	13
Figure S8: Five-day composite images of satellite-derived surface chlorophyll <i>a</i> in Baffin Bay during April–August 2016	14

Table S1: Linear measurements, biovolume, and carbon biomass^a of the taxa observed in Baffin Bay

Genus and species	n	D (μm)	PA (μm)	AA (μm)	TA (μm)	Shape	Mean volume (μm ³)	Mean carbon biomass (pg cell ⁻¹)
<i>Attheya</i> spp.	20	- ^b	4.3–22.4 [10.7]	3.5–12.2 [6.2]	2.8–9.7 [5.0]	Elliptical cylinder	236	28
<i>Bacterosira bathyomphala</i>	12	19.5–22.8 [21.0]	11.6–27.3 [16.9]	-	-	Cylinder	5,959	329
<i>C. decipiens</i>	18	-	16.8–36.2 [23.6]	18.3–70.5 [39.6]	14.1–54.3 [30.5]	Elliptical cylinder	24,836	973
<i>C. gelidus</i> (<i>C. socialis</i>)	18	-	4.6–13.7 [8.8]	4.2–10.5 [6.0]	2.1–5.3 [3.0]	Elliptical cylinder	123	17
<i>Eucampia groenlandica</i>	19	-	25.5–70.9 [40.4]	10.9–15.6 [13.3]	4.4–6.2 [5.3]	Elliptical cylinder	2,269	158
<i>Leptocylindrus danicus</i>	4	7.8–11.0 [8.8]	58.2–62.3 [60.8]	-	-	Cylinder	3,792	233
<i>Melosira arctica</i> (cell + spore)	22	18.7–26.5 [22.0]	18.6–29.8 [25.0]	-	-	Cylinder	9,839	482
<i>Porosira glacialis</i>	7	32.4–52.9 [44.2]	12.6–30.6 [20.9]	-	-	Cylinder	33,298	1,216
<i>Rhizosolenia hebetata</i> var. <i>hebetata/semispina</i>	3	13.5–21.3 [18.4]	589.0–850.0 [727.5]	-	-	Cylinder	210,852	4,946
<i>Thalassiosira anguste-lineata</i>	11	32.7–45.6 [39.4]	13.3–24.8 [19.0]	-	-	Cylinder	24,176	954
<i>T. antarctica</i> var. <i>borealis</i> (spore) ^c	10	-	-	-	-	Cylinder	7,067	374
<i>T. antarctica</i> var. <i>borealis/gravida</i> (cell)	20	16.0–42.0 [29.7]	14.9–29.1 [19.8]	-	-	Cylinder	14,722	654
<i>T. hyalina</i>	11	29.5–46.3 [39.7]	11.9–17.5 [15.1]	-	-	Cylinder	19,397	807
<i>T. nordenskiöldii</i>	22	15.3–19.9 [19.8]	12.2–22.4 [16.0]	-	-	Cylinder	5,062	291
<i>Pauliella taeniata</i>	41	-	6.0–13.8 [9.1]	16.8–40.0 [28.3]	4.9–11.6 [8.2]	Elliptical cylinder	1,709	127
<i>Ceratoneis closterium</i>	60	2.1–5.8 [3.7]	52.3–221.0 [96.6]	-	-	Spindle	671	63
<i>Entomoneis</i> spp.	7	-	17.5–41.7 [28.1]	49.2–182.6 [91.9]	9.8–36.5 [18.4]	Elliptical cylinder	53,535	1,745
<i>Fossula arctica</i>	23	-	5.0–9.0 [7.0]	11.0–29.0 [16.9]	2.3–6.1 [3.6]	Elliptical cylinder	355	39
<i>Fragilariopsis cylindrus</i>	41	-	1.0–5.0 [2.2]	4.0–42.0 [10.8]	1.0–5.0 [2.2]	Cuboid x 0.9	75	12
<i>F. oceanica</i>	24	-	3.3–8.0 [4.8]	12.0–29.0 [18.6]	2.8–8.0 [4.4]	Elliptical cylinder	346	38
<i>Fragilariopsis</i> spp. (10-20)	18	-	3.9–8.2 [6.5]	10.3–20.0 [15.3]	2.6–5.0 [3.8]	Elliptical cylinder	325	36
<i>Fragilariopsis</i> spp. (> 50)	18	-	3.5–6.6 [5.6]	21.9–57.8 [41.3]	5.4–14.3 [10.3]	Elliptical cylinder	2,034	145
<i>Gyrosigma / Pleurosigma</i> spp.	19	-	10.2–29.9 [20.8]	87.7–183.0 [131]	10.2–29.9 [20.8]	Elliptical cylinder	46,894	1,578
<i>Membraneis</i> spp.	4	-	33.7–37.8 [36.2]	66.9–82 [73.3]	22.3–27.3 [24.4]	Elliptical cylinder	51,014	1,682
<i>Navicula septentrionalis</i>	20	-	5.9–10.9 [9.1]	21.1–30.2 [28.1]	5.9–10.9 [9.1]	Elliptical cylinder	1,919	139
<i>N. vanhoeffenii</i>	19	-	6.4–16.5 [9.4]	29.8–64.7 [48.3]	6.4–16.5 [9.4]	Lanceolate cylinder x 0.85	2,696	180
<i>Navicula</i> spp. (20-50)	17	-	4.0–10.3 [7.6]	22.1–48.2 [36.5]	4.7–12.1 [8.9]	Elliptical cylinder	2,239	156
<i>Navicula</i> spp. (>50)	26	-	5.9–19.9 [11.1]	51.8–86.0 [62.7]	6.9–23.4 [13.0]	Elliptical cylinder	7,947	409
<i>Nitzschia frigida</i>	46	-	3.8–9.6 [6.5]	44.9–93 [61.0]	7.6–19.2 [13.1]	Lanceolate cylinder	3,631	226
<i>N. promare</i>	10	-	4.4–6.3 [5.3]	36.1–44.9 [40.6]	8.8–12.6 [10.6]	Prism on parallelogram-base x 1.15	1,361	107
<i>Nitzschia</i> spp. (>50)	15	-	2.7–11.7 [5.8]	61.5–205.0 [113.5]	5.3–23.4 [11.7]	Prism on parallelogram-base x 1.15	6,316	344
<i>Plagiotropis</i> spp.	7	-	10.6–23.2 [19.1]	38.3–68.9 [58.9]	10.6–19 [16.3]	Prism on parallelogram-base x 1.15	11,377	538
<i>Pseudo-nitzschia delicatissima</i>	55	-	1.3–3.4 [2.0]	40.1–86.0 [73.4]	1.8–4.5 [2.7]	Prism on parallelogram-base x 0.7	144	19
<i>Pseudo-nitzschia seriata</i>	48	-	2.3–5.9 [3.9]	48.5–87.4 [65.7]	3.0–7.8 [5.2]	Prism on parallelogram-base x 0.7	495	50
<i>Synedropsis hyperborea</i>	23	-	1.5–4.6 [2.8]	22.4–68.5 [44.1]	1.9–5.9 [3.6]	Elliptical cylinder	376	40

^a Range and mean (in brackets) are indicated together for the linear measurements. Shapes were used to estimate a mean volume from linear dimensions. The carbon biomass was estimated from the mean volume of each taxon, where n = number of observations, D = diameter, PA = pervalvar axis, AA = apical axis, and TA = transapical axis.

^b The absence of measurements is due to the shape of the cell (e.g., for cylindrical cells, only D and PA are necessary to calculate the biovolume, whereas for elliptical cylinders three measurements are needed).

^c Because *Thalassiosira antarctica* var. *borealis* resting spores were usually observed within the cell, the ratio between the surface of the spore and the surface of the cell was measured to derive the biovolume of the spores ($S_{\text{spore}} = 0.48 \times S_{\text{cell}}$; n = 10).

Table S2: Functional trait data^a for the taxa observed in Baffin Bay

Taxa	Quantitative trait		Binary trait ^b		Continuous trait (from 0 to 1) ^b			
	ESD ^c	S/V ^c	T _{opt} ^d	IBP ^d	Spikes	Silicified	Spores	Colonies
<i>Attheya septentrionalis/A. longicornis</i>	8	1.00	2.00	1.00	1.00	0.00	0.00	0.5
<i>Bacterosira bathyomphala</i>	22	0.30	4.00	0.00	0.00	0.00	1.00	1.00
<i>Chaetoceros gelidus</i>	6	1.24	8.00	0.00	1.00	0.00	1.00	1.00
<i>Chaetoceros decipiens</i>	36	0.18	14.00	0.00	1.00	1.00	0.00	1.00
<i>Ceratoneis closterium</i>	11	0.83	9.00	0.00	0.00	0.00	0.50	0.0
<i>Eucampia groelandica</i>	16	0.57	4.00	0.00	1.00	0.00	0.00	1.00
<i>Fragilariopsis cylindrus</i>	5	1.26	5.00	1.00	0.00	1.00	0.00	1.00
<i>F. oceanica</i>	9	0.85	5.00	1.00	0.00	1.00	1.00	1.00
<i>Fossula arctica</i>	9	0.90	5.00	1.00	0.00	1.00	1.00	1.00
<i>Leptocylindrus danicus</i>	19	0.48	28.00	0.00	0.00	0.00	1.00	0.50
<i>Navicula vanhoeffenii</i>	17	0.58	4.00	0.00	0.00	0.50	0.00	1.00
<i>N. septentrionalis</i>	15	0.49	4.00	0.00	0.00	0.50	1.00	1.00
<i>Pauliella taeniata</i>	15	0.52	4.00	0.00	0.00	0.50	1.00	1.00
<i>Nitzschia frigida</i>	19	0.25	1.00	0.00	0.00	1.00	0.00	1.00
<i>Pseudo-nitzschia seriata</i>	10	0.57	23.00	0.00	0.00	0.00	0.00	1.00
<i>P. delicatissima</i>	7	1.14	23.00	0.00	0.00	0.00	0.00	1.00
<i>Rhizosolenia hebetata</i> f. <i>semispina</i>	74	0.20	10.00	0.00	1.00	1.00	0.50	0.50
<i>Thalassiosira antarctica</i> var. <i>borealis</i>	30	0.22	13.00	0.00	1.00	1.00	1.00	1.00
<i>T. nordenskiöldii</i>	21	0.32	13.00	0.00	1.00	1.00	1.00	1.00
<i>T. hyalina</i>	33	0.22	2.00	0.00	1.00	1.00	1.00	1.00
<i>Melosira arctica</i>	27	0.25	5.00 ^e	1.00 ^f	0.00	1.00	1.00	1.00

^a Abbreviations refer to equivalent spherical diameter (ESD), surface area to volume ratio (S/V), optimal temperature for growth (T_{opt}), and ability to produce ice-binding proteins (IBP). ‘Spikes’ refers to the presence or absence of long, sharp projections such as setae, spines, horns and cellular processes. ‘Silicified’ refers to the degree of silicification, qualitatively based on examination of SEM images. ‘Spores’ refers to the propensity to form resting spores. ‘Colonial’ refers to the ability to form colonies.

^b Binary and continuous traits were coded using a ‘fuzzy code’ (Chevene et al., 1994), which allows species to exhibit a trait to a certain degree. Continuous traits were arbitrarily scaled to a value between 0 and 1 (i.e., lowest (= 0), intermediate (0.5), and highest (= 1) probability of species having that trait.

^c ESD and S/V data come from this study. Other trait data were retrieved from Fragoso et al. (2018) who conducted an extensive literature search for ecological strategies, life history and morphological traits of diatom species. Details about the traits and how they are encoded can also be found in Fragoso et al. (2018). We added the species *Melosira arctica* (see the bibliography below) which was observed in our study, but not in Fragoso et al. (2018).

^d As it was difficult to find information for the traits T_{opt} and IBP for every species, some species were grouped based on trait similarities (i.e., cell morphology; e.g., *Thalassiosira antarctica* var. *borealis* and *T. nordenskiöldii* are both highly silicified, form colonies, share similar shape, and produce resting spores), and one single value for T_{opt} and IBP was given to the species belonging to the same group.

^e The optimal temperature for *Melosira arctica* growth was found in Spilling and Markager (2008).

^f The ability of *Melosira arctica* to produce ice-binding proteins was highlighted by Krembs et al. (2011).

Table S3: Summary of the environmental and biological data at the 29 stations

Metadata			Environmental data ^a										Biological data ^b									
Station	Longitude	Latitude	Date of sampling (year-month-day)	Depth of the SCM (m)	DOW50 (d)	SIC	hBD (m)	Ze (m)	ANP (%)	[NO ₃ ⁻] (mmol m ⁻²)	[H ₄ SiO ₄] (mmol m ⁻²)	[PO ₄ ³⁻] (mmol m ⁻²)	[Chl <i>a</i>] (mg m ⁻²)	[BSi] (mmol m ⁻²)	[Chl <i>c3</i>] (mg m ⁻²)	[Phaeo <i>a</i>] (mg m ⁻²)	∫ρSi (mmol m ⁻² d ⁻¹)	∫VSi (d ⁻¹)	Abundance (cells L ⁻¹)		C Biomass (µg C L ⁻¹)	
																			Surface	SCM	Surface	SCM
100	-56.79	68.499	2016-06-09	40	15	0.00	29	41	11.8	0.0	17.6	2.1	34.7	32.7	5.0	8.0	0.6	1.5	33,800	34,480	5.4	9.4
102	-57.48	68.497	2016-06-10	40	15	0.00	41	33	7.2	4.0	42.1	5.0	90.2	45.6	11.1	14.3	0.3	0.6	-	47,960	-	16.7
107	-59.18	68.498	2016-06-11	- ^c	-15	0.97	21	13	9.6	50.2	85.7	7.6	63.3	16.3	3.8	3.8	1.2	5.1	-	-	-	-
110	-60.17	68.534	2016-06-12	-	-23	1.00	26	21	20.7	145.1	137.0	17.4	29.7	15.4	2.2	1.7	0.7	3.3	-	-	-	-
115	-61.36	68.456	2016-06-13	30	-20	0.93	24	31	63.0	103.6	244.5	22.5	12.9	10.3	1.3	1.0	0.4	3.4	24,696	1-764	1.4	0.5
201	-59.95	68.633	2016-06-14	40	-18	0.98	26	31	21.0	151.7	151.9	17.6	34.7	20.5	3.0	1.5	0.6	2.3	19,656	13,356	3.7	1.5
204	-59.26	68.708	2016-06-15	15	-12	0.93	18	22.5	10.7	25.2	31.9	4.8	66.9	35.4	3.6	6.0	1.9	2.1	915,594	463,680	93.6	122.7
207	-58.53	68.794	2016-06-16	15	6	0.41	14	22.5	1.6	0.8	23.1	1.7	77.3	61.2	6.3	6.2	1.7	1.5	78,627	119,448	26.5	55.5
300	-56.79	68.999	2016-06-17	44	31	0.00	38	-	9.4	7.5	35.2	5.1	100.7	58.4	17.4	12.2	2.0	3.2	16,128	34,776	6.8	9.3
309	-58.74	69.000	2016-06-18	15	2	0.00	19	29.5	2.2	1.7	19.0	1.3	73.6	63.4	3.4	5.1	3.0	2.1	256,536	429,015	36.2	56.5
312	-59.56	69.012	2016-06-19	15	-8	1.00	18	15.8	17.7	49.3	72.7	8.3	44.3	32.3	3.7	4.3	2.2	3.8	18,900	86,436	3.4	16.5
318	-60.95	69.007	2016-06-20	-	-6	0.99	21	27.5	24.4	110.0	111.3	14.1	29.5	18.4	3.0	1.5	0.5	2.2	8,920	-	1.2	-
324	-62.36	68.996	2016-06-21	20	-20	1.00	25	21.5	41.6	95.8	178.5	19.1	38.3	15.4	2.9	1.6	0.7	3.5	48,132	27,468	5.7	2.9
403	-61.60	68.031	2016-06-25	-	-17	0.86	26	40.5	44.3	139.3	222.2	22.6	5.5	7.9	0.4	0.7	0.3	3.5	18,680	-	1.2	-
405	-61.08	68.094	2016-06-26	-	-9	1.00	21	-	44.3	89.9	176.1	16.7	-	11.5	-	-	-	-	-	-	-	-
409	-59.99	68.106	2016-06-26	-	-14	1.00	15	27	17.2	42.0	87.3	9.8	43.2	17.4	3.2	1.9	1.1	4.5	30,000	-	4.2	-
413	-58.97	68.123	2016-06-27	30	-2	0.77	21	-	9.3	28.9	51.3	6.4	30.9	30.6	2.0	11.6	-	-	21,672	18,900	7.1	2.5
418	-57.77	68.114	2016-06-28	30	23	0.00	18	43	2.9	0.8	12.3	2.0	21.4	25.8	1.6	4.5	0.8	3.7	1,008	1,764	0.1	0.1
507	-59.12	70.009	2016-06-30	12	8	0.00	15	20	10.2	3.8	6.3	3.1	100.5	74.6	1.4	18.9	2.4	1.8	623,952	610,344	149.0	210.0
512	-60.36	70.003	2016-07-01	15	3	0.00	11	21	4.3	2.7	7.0	1.0	127.4	79.6	16.9	5.5	1.9	1.4	204,624	483,840	70.3	135.7
519	-62.42	70.017	2016-07-02	-	-2	0.84	14	34.5	25.8	61.3	108.8	8.8	14.2	9.7	0.9	1.5	-	-	-	-	-	-
600	-63.99	70.511	2016-07-03	-	-10	0.91	21	28	45.3	46.6	149.8	13.0	36.3	17.3	2.6	2.5	-	-	61,680	-	8.0	-
605	-62.52	70.503	2016-07-04	20	0	0.17	17	41.5	24.5	37.7	124.4	9.6	28.9	13.6	1.5	1.5	-	-	30,492	43,848	5.9	2.4
615	-59.52	70.499	2016-07-05	30	12	0.00	16	30.5	11.0	0.0	20.2	1.6	164.4	27.2	35.5	5.9	1.4	3.8	8,064	30,744	2.4	10.3
604.5	-62.63	70.502	2016-07-06	-	2	0.00	15	44.5	40.3	21.2	84.9	8.2	26.4	15.2	1.0	2.0	0.4	2.1	-	-	-	-
703	-58.72	69.500	2016-07-07	35	23	0.00	18	52	9.0	61.4	47.4	7.6	36.7	29.7	2.2	2.5	-	-	18,396	10,584	10.5	1.3
707	-59.80	69.512	2016-07-08	35	10	0.00	16	32.5	20.2	0.7	9.6	3.1	71.9	40.6	7.1	4.4	-	-	184,968	39,312	25.3	2.6
713	-61.58	69.501	2016-07-09	20	6	0.00	15	30.5	27.5	3.2	36.0	4.4	40.2	20.9	4.1	1.7	-	-	13,608	7,812	1.6	0.4
719	-63.23	69.501	2016-07-10	21	-2	0.60	16	26	50.8	31.6	129.4	10.4	48.0	15.0	2.1	2.5	0.8	3.5	27,216	105,840	5.7	9.5

^a Nutrients were integrated down to the depth of the equivalent mixed layer hBD.

^b Pigments and BSi data were integrated down to 80 m, because at that depth, almost all Chl *a* profiles were sufficiently close to 0, indicating that no significant biomass was missed.; ρSi and VSi were integrated down to the depth at which 0.1 % of the surface PAR remained.

^c Data not presentable or not available. The depth of the SCM is only shown for the stations where diatoms were counted at the depth of the subsurface chlorophyll *a* maximum. ρSi, and VSi were not measured at all of the 29 stations, explaining the missing data.

Table S4: Diatoms observed in Baffin Bay during the Green Edge expedition

	Taxonomy (size)	Cell abundance (cells L ⁻¹)		Occurrence (%) ^a	
		Mean	Maximum		
Centric	<i>Attheya longicornis</i>	2,761	35,784	63	
	<i>A. septentrionalis</i>	239	1,983	35	
	<i>Bacterosira bathyomphala</i>	99	1,640	12	
	<i>Chaetoceros atlanticus</i>	6	273	2	
	<i>C. borealis</i>	92	3,024	5	
	<i>C. concavicornis</i>	82	3,528	2	
	<i>C. cf. debilis</i>	3,198	76,104	19	
	<i>C. decipiens</i>	1,916	20,870	47	
	<i>C. gelidus</i>	42,013	526,742	40	
	<i>Chaetoceros</i> spp. (< 10 µm)	601	9,480	14	
	<i>Chaetoceros</i> spp. (10–20 µm)	372	5,544	23	
	<i>Chaetoceros</i> spp. (20–50 µm)	534	5,544	33	
	<i>Chaetoceros</i> spp. (hypnospores)	6	252	2	
	<i>Coscinodiscus cf. centralis</i>	12	504	2	
	<i>cf. Dactyliosolen</i> spp.	29	1,260	2	
	<i>Eucampia groenlandica</i>	1,085	8,568	35	
	<i>Leptocylindrus danicus</i>	316	10,584	9	
	<i>Melosira arctica</i>	441	5,040	16	
	<i>M. arctica</i> spores	5,060	124,488	33	
	<i>Porosira glacialis</i>	136	2,016	21	
	<i>Rhizosolenia hebetata</i> var. <i>hebetata</i>	6	252	2	
	<i>R. hebetata</i> var. <i>semispina</i>	24	504	12	
	<i>Skeletonema costatum</i> -like species	59	2,520	2	
	<i>Thalassiosira anguste-lineata</i>	107	1,640	12	
	<i>T. antarctica</i> var. <i>borealis</i> (spores)	106	3,024	9	
	<i>T. bioculata</i> (cells + spores)	35	504	9	
	<i>T. antarctica</i> var. <i>borealis/gravida</i>	7,721	68,040	51	
	<i>T. hyalina</i>	581	9,576	16	
	<i>T. nordenskiöldii</i>	2,216	18,574	37	
	<i>Thalassiosira</i> spp. (5–10 µm)	23	756	5	
	<i>Thalassiosira</i> spp. (10–20 µm)	1,130	12,096	56	
	<i>Thalassiosira</i> spp. (20–50 µm)	4,330	58,968	74	
	<i>Thalassiosira</i> spp. (> 50 µm)	583	9,576	42	
	Centric diatom spp. (2–10 µm)	211	5,600	9	
	Centric diatom spp. (10–20 µm)	129	2,520	21	
	Centric diatom spp. (20–50 µm)	288	2,016	35	
	Centric diatom spp. (> 50 µm)	32	522	12	
	Pennate	<i>Pauliella taeniata</i>	199	7,560	5
		<i>Ceratoneis closterium</i>	7,051	75,096	95
		<i>Entomoneis</i> spp.	216	4,040	26
<i>Fossula arctica</i>		1,979	41,832	16	
<i>Fragilariopsis cylindrus</i>		637	15,876	21	
<i>F. oceanica</i> (cells)		2,877	65,520	14	
<i>F. oceanica</i> (spores)		680	29,232	2	
<i>Fragilariopsis</i> spp. (10–20 µm)		8,553	231,861	35	
<i>Fragilariopsis</i> spp. (20–50 µm)		2,058	30,720	28	
<i>Gyrosigma/Pleurosigma</i> spp.		30	504	14	
<i>Licmophora</i> spp.		12	504	2	
<i>Membraneis</i> spp.		8	120	9	
<i>Navicula pelagica</i>		61	1,855	5	
<i>N. septentrionalis</i>		798	14,112	14	
<i>N. vanhoeffenii</i>		49	1,600	5	
<i>Navicula</i> spp. (20–50 µm)		725	8,064	42	
<i>Navicula</i> spp. (> 50 µm)		204	2,520	30	
<i>Nitzschia frigida</i>		1,993	30,744	30	
<i>N. promare</i>		55	1,080	9	
<i>Nitzschia</i> spp. (20–50 µm)		19	504	7	
<i>Nitzschia</i> spp. (> 50 µm)		28	252	21	
<i>Pseudogomphonema arcticum</i> ^b		- ^b	-	-	
<i>Pseudo-nitzschia delicatissima</i>		6,645	83,160	91	
<i>Pseudo-nitzschia seriatia</i>		299	2,920	26	
<i>Synedropsis hyperborea</i>		321	5,200	21	
<i>Thalassionema nitzschioides</i>		4	120	5	
Pennate diatom spp. (10–20 µm)		3,305	45,864	70	
Pennate diatom spp. (20–50 µm)		3,128	17,136	91	
Pennate diatom spp. (> 50 µm)		926	7,056	53	

^a Percent of all samples in which the taxon occurred

^b Observed by scanning electron microscopy only

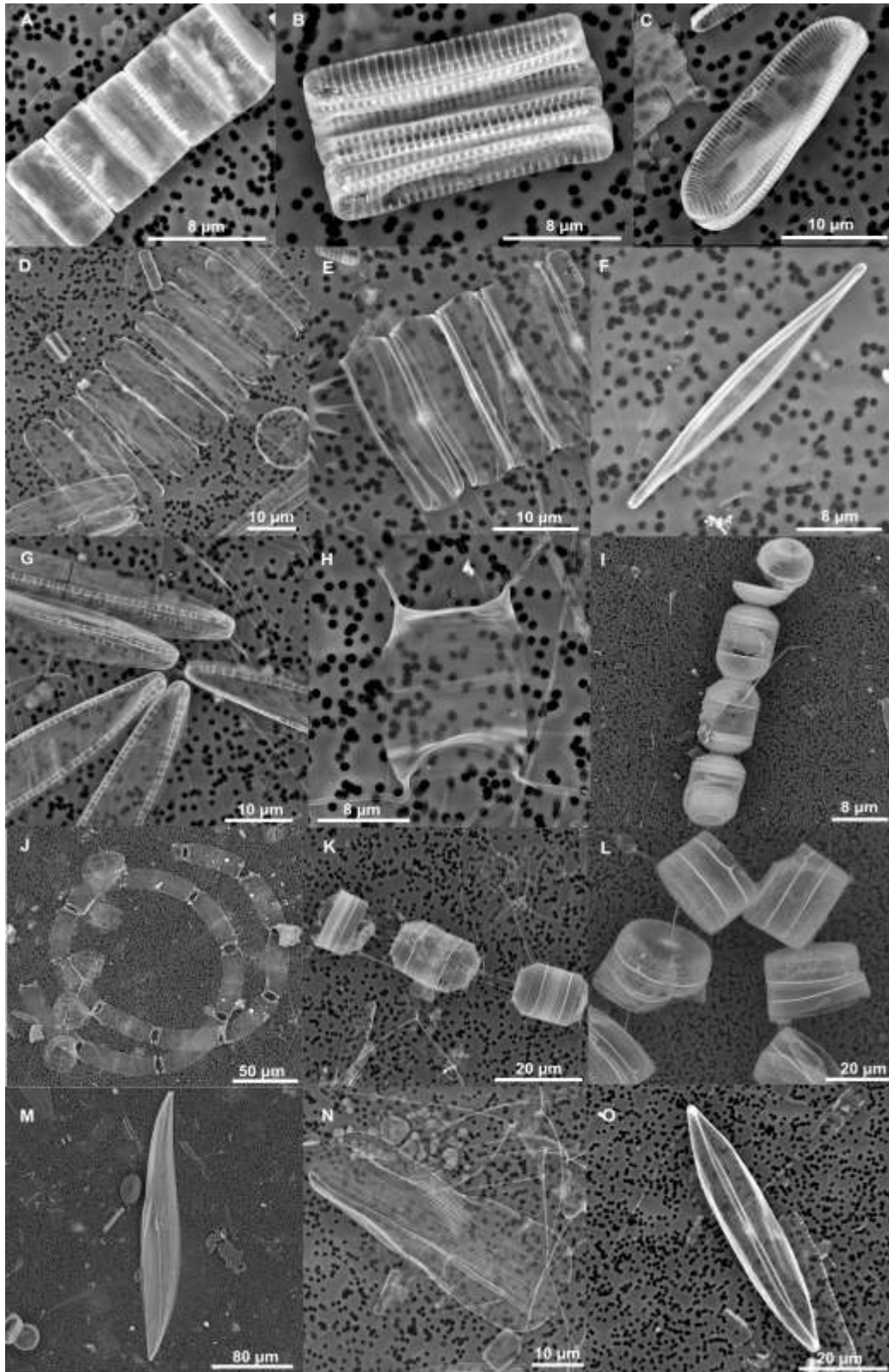


Figure S1. Selection of diatom species observed by scanning electron microscopy

Three samples (from stations 409, 507, and 600) were examined by scanning electron microscopy to help identify the diversity of species prior to counting under a light microscope: (A) *Fossilula arctica*, (B) *Fragilariopsis cylindrus*, (C) *Fragilariopsis oceanica*, (D) *Navicula vanhoeffenii*, (E) *Pauliella taeniata*, (F) *Synedropsis hyperborea*, (G) *Nitzschia frigida*, (H) *Chaetoceros gelidus*, (I) *Melosira arctica*, (J) *Eucampia groenlandica*, (K) *Thalassiosira nordenskiöldii*, (L) *Thalassiosira antarctica* var. *borealis*, (M) *Pleurosigma* sp., (N) *Entomoneis* sp., and (O) *Navicula* sp.

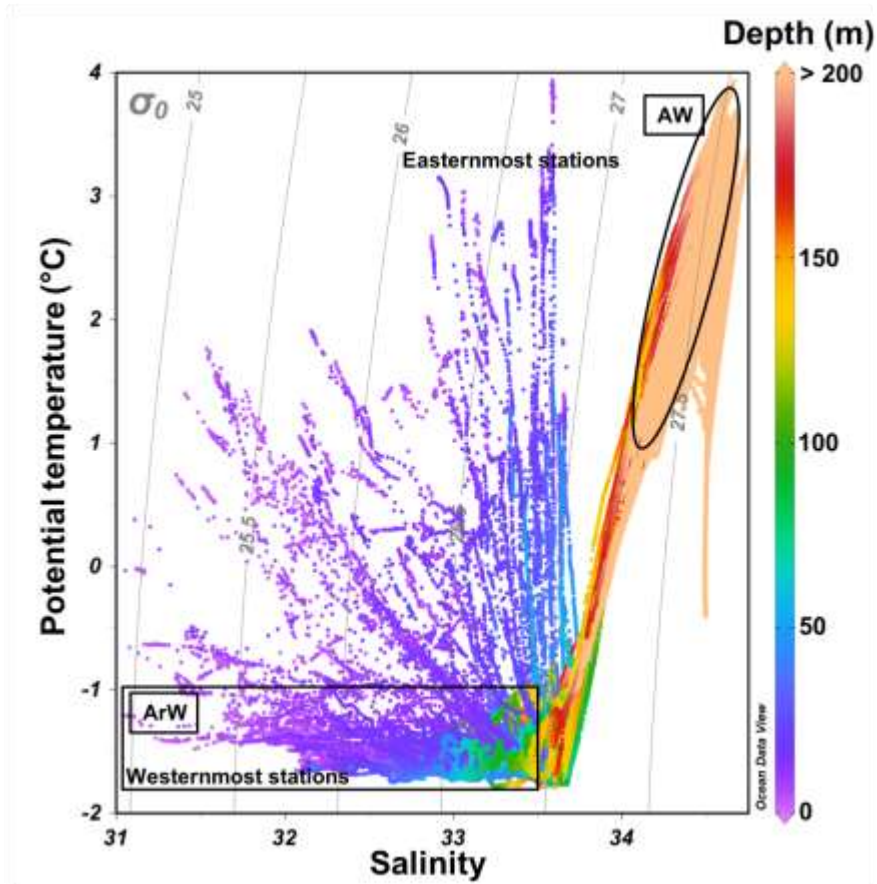


Figure S2. T-S diagram for all of the stations

Grey lines represent the isopycnal lines. According to the water masses defined by Tang et al. (2004) and modified by Randelhoff et al. (2019), we identify the Arctic waters (ArW) by $T < -1^\circ\text{C}$ and $S < 33.5 \text{ g kg}^{-1}$, and the Atlantic waters (AW) by $T > 1^\circ\text{C}$ and $S > 34 \text{ g kg}^{-1}$. In ArW, we calculated an ANP signature $> 20\%$ (up to 60%), whereas in AW, ANP $< 10\%$. The T-S diagrams are clearly different between the westernmost and easternmost stations, especially in the first 50 m, showing the west-east gradient in water masses.

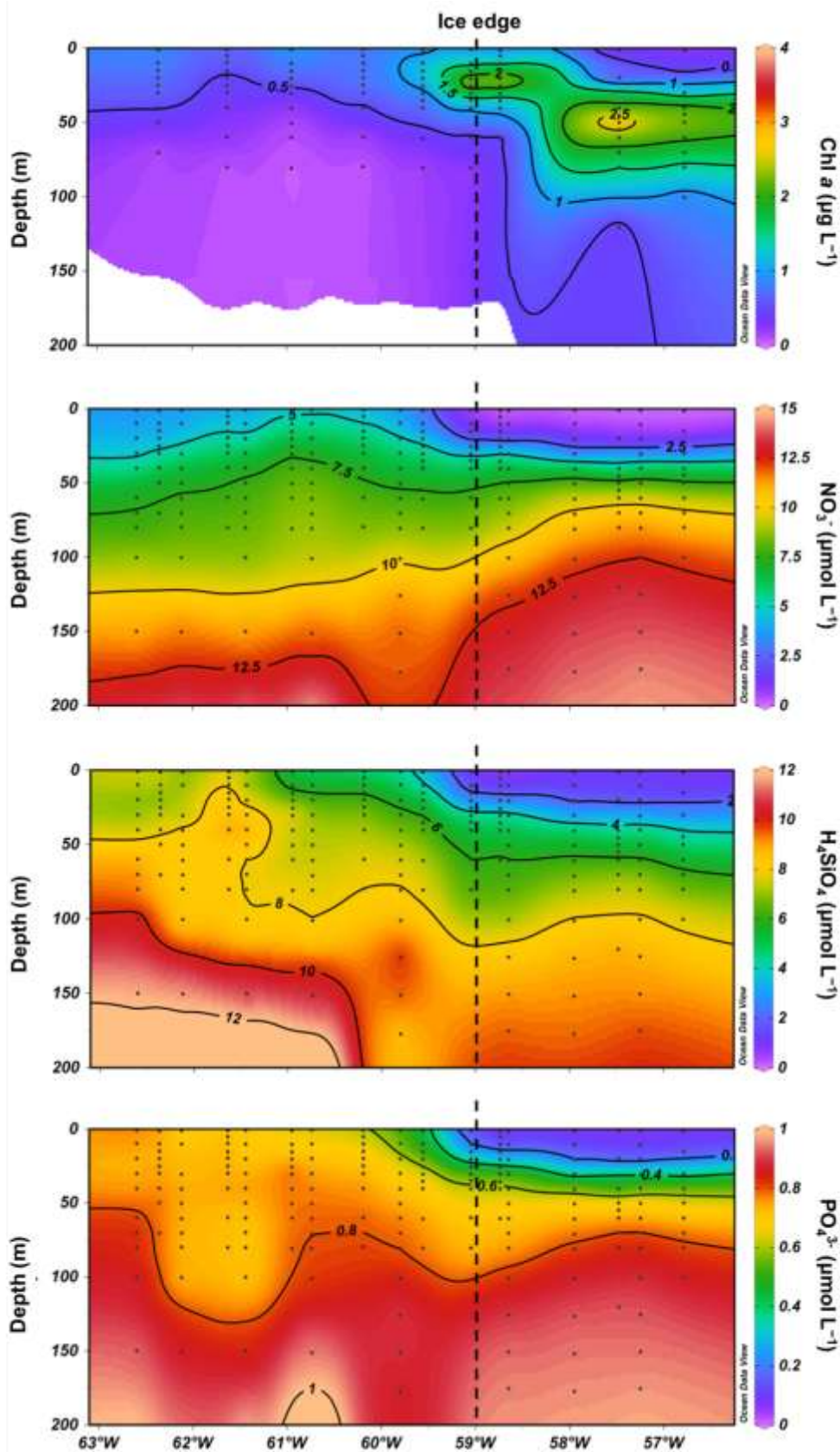


Figure S3. Vertical distribution of concentrations of chlorophyll *a* and nutrients for transect T3

Transect T3 is shown, as it well represents nutrient distributions (nitrate, orthosilicic acid, and phosphate) observed on other transects. The vertical dashed line at 59°W corresponds to the location of the ice edge (SIC = 0.5).

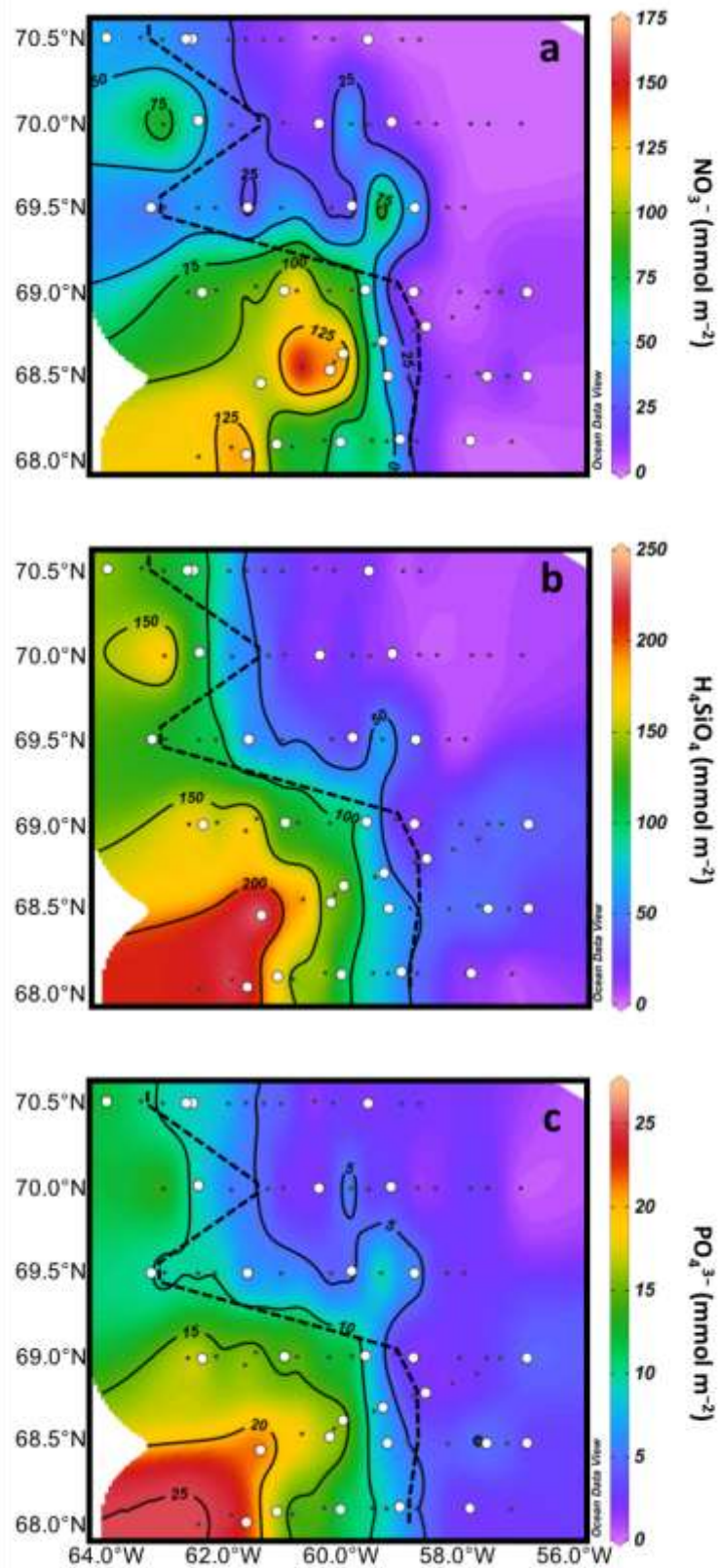


Figure S4. Integrated nutrient concentrations over the depth of the equivalent mixed layer (hBD)

The following nutrient concentrations are presented: nitrate (a), orthosilicic acid (b), and phosphate (c). The dashed black lines correspond to the ice edge (SIC = 0.5).

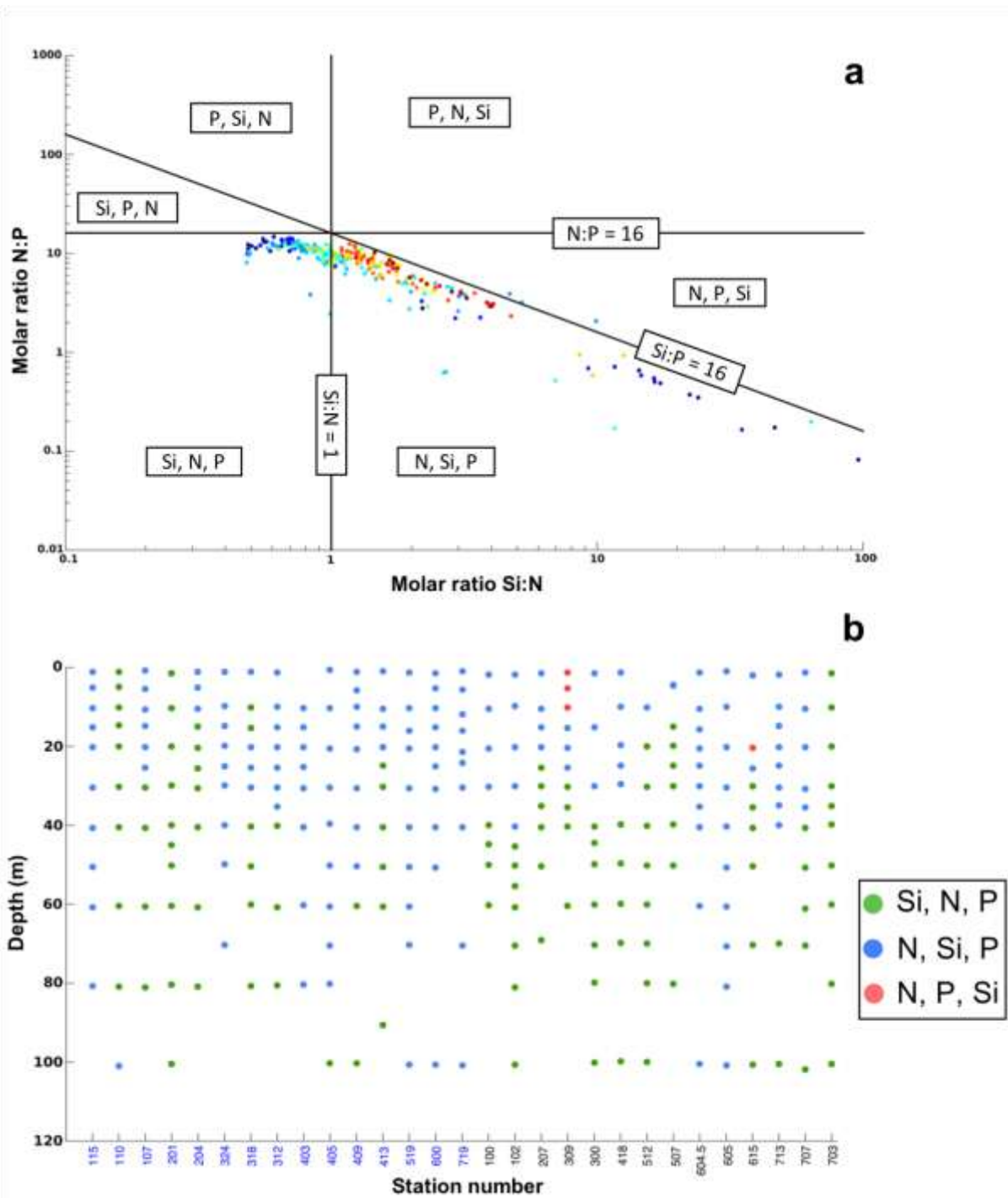


Figure S5. Potential limiting nutrients in rank order (most limiting first) based on nutrient ratios

a) Si:N:P molar ratios for all data collected between the surface and 120-m depth. In each area, as delimited by the Redfield et al. (1963) and Brzezinski (1985) ratios (Si:N:P = 16:16:1), the potential limiting nutrients are reported in rank order, with the most limiting nutrient listed first. Data points are colored according to station longitude, with blue circles corresponding to easternmost stations and red circles to westernmost stations. (b) Synthesis depiction by depth and station of the potential limiting nutrients color-coded to indicate rank order (see inset box). The station numbers for ice-covered locations are indicated in blue on the bottom axis.

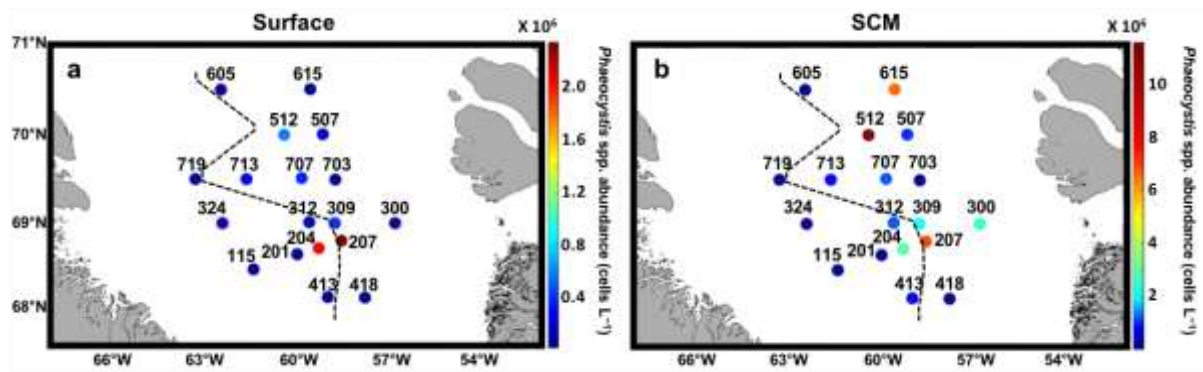


Figure S6. Abundance of *Phaeocystis* spp. in surface waters and at the subsurface chlorophyll *a* maximum

Color-coded abundance of *Phaeocystis* spp. in surface waters (a) and at the subsurface chlorophyll *a* maximum (SCM) (b). The dashed black lines indicate the ice edge (SIC = 0.5).

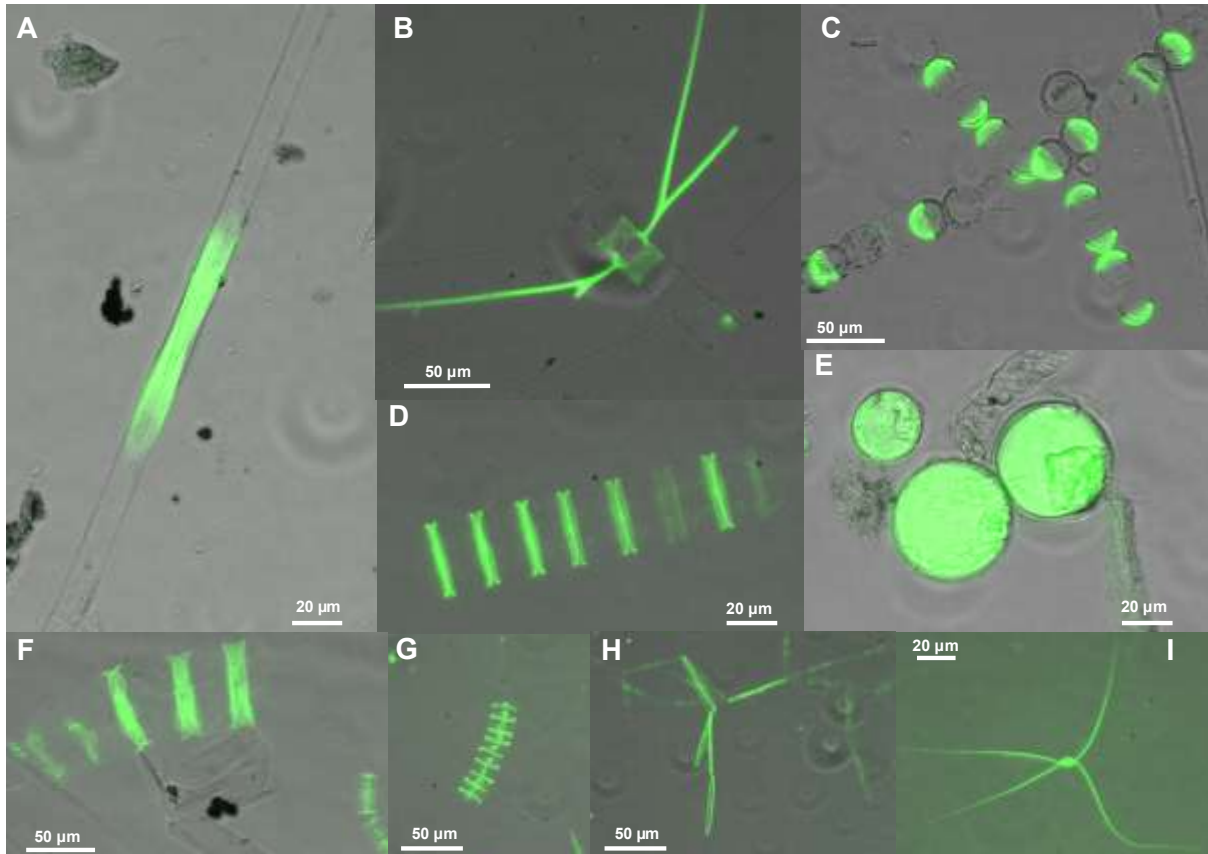


Figure S7. Examples of actively silicifying diatoms labelled with the fluorescent dye PDMPO

Micrographs are composites of epifluorescent and light microscopy images. (A) *Rhizosolenia hebetata* var. *semispina*, (B) *Chaetoceros decipiens*, (C) *Melosira arctica* spores, (D) *Navicula vanhoeffenii*, (E) *Thalassiosira antarctica* var. *borealis*, (F) *Entomoneis* sp., (G) *Fragilariopsis* sp., (H) *Nitzschia frigida*, and (I) *Chaetoceros* sp.

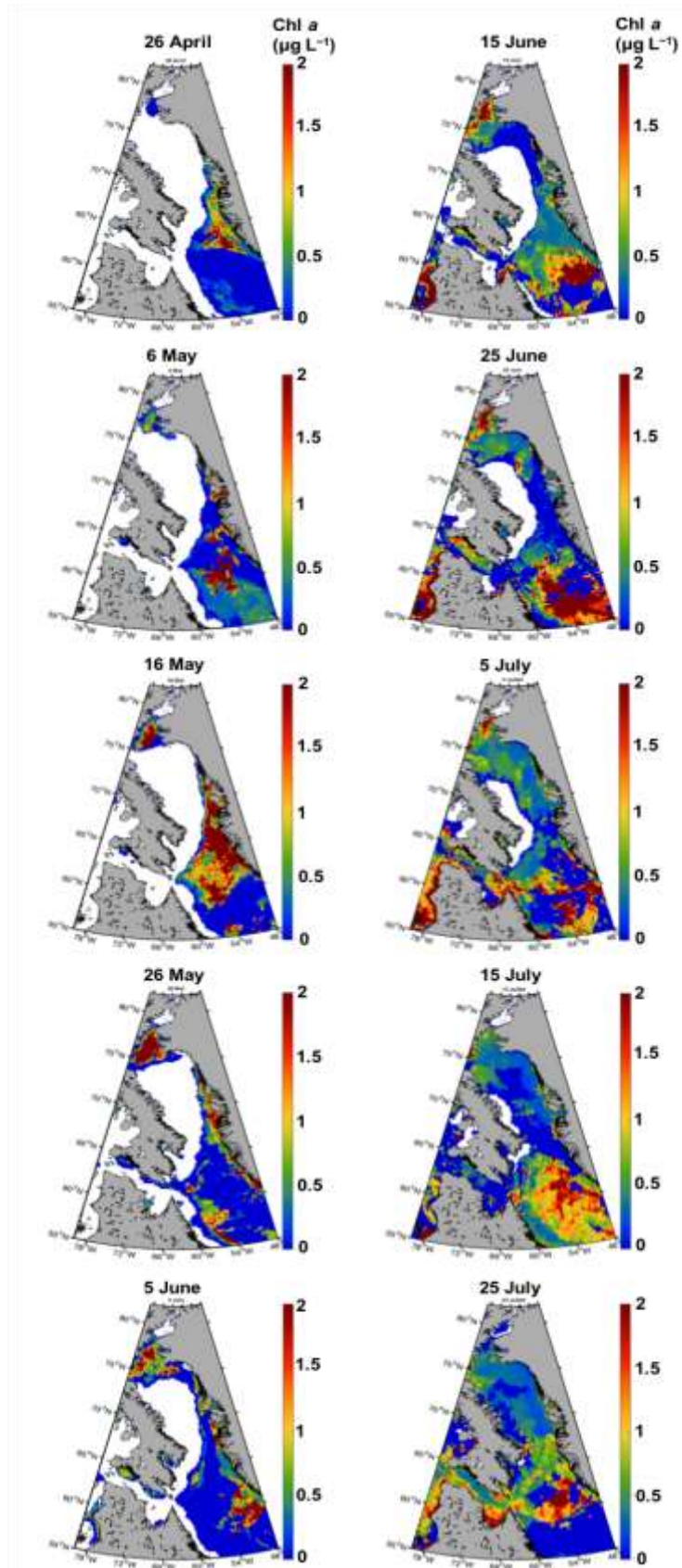


Figure S8, Five-day composite images of satellite-derived surface chlorophyll *a* in Baffin Bay during April–August 2016

The white area in these MODIS level 3 products corresponds to locations where sea ice concentration was > 0.5 .

References

- Brzezinski MA. 1985. The Si:C:N ratio of marine diatoms: interspecific variability and the effect of some environmental variables. *J Phycol* **21**(3): 347–357. doi: 10.1111/j.0022-3646.1985.00347.x
- Chevène F, Doledec S, Chessel D. 1994. A fuzzy coding approach for the analysis of long-term ecological data. *Freshw Biol* **31**(3): 295–309. doi: 10.1111/j.1365-2427.1994.tb01742.x
- Fragoso GM, Poulton AJ, Yashayaev IM, Head EJH, Johnsen G, Purdie DA. 2018. Diatom biogeography from the Labrador Sea revealed through a trait-based approach. *Front Mar Sci* **5**. doi: 10.3389/fmars.2018.00297
- Krembs C, Eicken H, Deming JW. 2011. Exopolymer alteration of physical properties of sea ice and implications for ice habitability and biogeochemistry in a warmer Arctic. *Proc Natl Acad Sci* **108**, 3653–3658. <https://doi.org/10.1073/pnas.1100701108>
- Randelhoff A, Oziel L, Massicotte P, Bécu G, Galí M, Lacour L, Dumont D, Vladioiu A, Marec C, Bruyant F, et al. 2019. The evolution of light and vertical mixing across a phytoplankton ice-edge bloom. *Elem Sci Anth* **7**(1): 20. doi: 10.1525/elementa.357
- Redfield AC, Ketchum BH, Richards FA. 1963. The influence of organisms on the composition of seawater. *The Sea*: 26–77. New York.
- Spilling K, Markager S, 2008. Ecophysiological growth characteristics and modeling of the onset of the spring bloom in the Baltic Sea. *J Mar Syst* **73**: 323–337. <https://doi.org/10.1016/j.jmarsys.2006.10.012>
- Tang CCL, Ross CK, Yao T, Petrie B, DeTracey BM, Dunlap E. 2004. The circulation, water masses and sea-ice of Baffin Bay. *Prog Oceanogr* **63**(4): 183–228. doi: 10.1016/j.pocean.2004.09.005